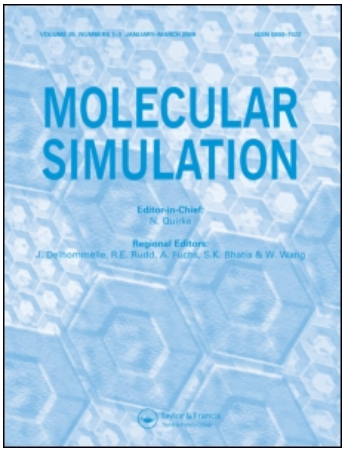

Molecular Simulation
Publication details, including instructions for authors and subscription information:
http://www.informaworld.com/smpp/title~content=t713644482

Adsorption equilibrium in one-dimensional molecular sieve: a study of force fields effect on linear alkanes molecules

Sebastiao M. P. Lucena[a]; Célio L. Cavalcante Jr[a]
[a] Grupo de Pesquisa em Separação por Adsorção (GPSA), Departamento de Engenharia Química, Universidade Federal do Ceará, Fortaleza, Ceará, Brazil

To cite this Article Lucena, Sebastiao M. P. and Cavalcante Jr, Célio L.(2008) 'Adsorption equilibrium in one-dimensional molecular sieve: a study of force fields effect on linear alkanes molecules', Molecular Simulation, 34: 10, 1337 — 1349
To link to this Article: DOI: 10.1080/08927020802301896
URL: http://dx.doi.org/10.1080/08927020802301896

Molecular Simulation
Vol. 34, Nos. 10–15, September – December 2008, 1337–1349

Taylor & Francis
Taylor & Francis Group

Adsorption equilibrium in one-dimensional molecular sieve: a study of force fields effect on linear alkanes molecules

Sebastiao M.P. Lucena* and Célio L. Cavalcante Jr[1]

Grupo de Pesquisa em Separação por Adsorção (GPSA), Departamento de Engenharia Química, Universidade Federal do Ceará, Fortaleza, Ceará, Brazil

(*Received 31 January 2008; final version received 24 June 2008*)

The effect of different force fields (united atom and all-atom) has been investigated on the adsorption of linear hydrocarbon molecules in $AlPO_4$-5 molecular sieve using grand canonical Monte Carlo (GCMC) simulations of *n*-hexane, *n*-pentane and *n*-butane. Adsorption isotherms and structural analysis were performed for linear alkanes and compared with reported experimental data. We show that the modulation between wide and narrow regions in $AlPO_4$-5 and the strong interaction between terminal methyl groups and oxygen atoms of the wide regions drive position and adsorption sites. Discrepancies in the positioning of *n*-pentane molecules suggest that the force field choice affects considerably *n*-pentane while *n*-hexane and *n*-butane presented lower sensibility. The force fields difference of sensibilities among the linear molecules seems to be associated with the critical geometric condition identified by Yashonath and Santikary and denominated 'levitation effect'. The molecules of *n*-pentane in $AlPO_4$-5 have dimensions that result in a levitation ratio (γ) close to unity. As previously shown for cyclic molecules, proper care should be taken in the choice of the force field when the guest–host size ratio of linear molecules is near the value defined for the levitation effect.

Keywords: aluminophosphates; alkane adsorption; linear adsorption; Monte Carlo simulation; levitation effect

1. Introduction

One of the main applications of the adsorption separation processes is the separation of *n*-paraffins from branched and cyclic alkanes [1,2]. In the Universal Oil Products Company (UOP) Molex process, *n*-paraffins from kerosene streams are separated from iso and cycle-paraffins and used as feedstock for the linear alkylbenzene sulphonate production [3]. In the Total Isomerization Process (TIP) from Shell/UOP a nonlinear paraffin rich stream is produced to increase gasoline octane number [4].

Studies about the behaviour of linear molecules in molecular sieves can contribute to the development of new adsorbents or the improvement of current processes. Determination of positioning and adsorption sites of these molecules is a good example on how molecular simulation can help to improve our understanding of confined molecular fluids. This subject is particularly controversial in the adsorption studies of linear alkanes in alumino-phosphated molecular sieve $AlPO_4$-5.

Newalkar et al. [5,6], Chiang et al. [7], Cavalcante et al. [8], Janchen et al. [9] and Eder and Lercher [10] have done experimental studies of hydrocarbons adsorption in aluminophosphate molecular sieves. For linear alkanes, Newalkar et al. [5,6] concluded, based on isosteric heats variation with loading, that *n*-pentane and *n*-hexane reside along the channels, parallel to the *c*-axis. The sorbate–sorbate interactions are minimum and limited to the terminal methyl groups. The saturation sorption capacity was about 1 molecule/unit cell (1.1 and 1.27 molecules/unit cell for *n*-hexane and *n*-pentane, respectively). According to the authors, in the saturation, the molecules may adsorb in a twisted configuration. This conclusion comes from the fact that the length of *n*-pentane and *n*-hexane molecules were estimated as 9.03 and 10 Å, respectively, and the length of the pore of $AlPO_4$-5 is only 8.45 Å. Chiang et al. [7] studied *n*-hexane adsorption and presented similar conclusions about the need of the *n*-hexane to assume a twisted position. Neither of these studies make reference to the adsorption sites.

Molecular simulation studies for these systems were performed by Maris et al. [11], Fox and Bates [12] and Bhide and Yashonath [13]. Maris et al. [11] studied the sorption of methane, ethane, propane, butane and *n*-pentane in $AlPO_4$-5. They concluded that the molecules of methane, ethane and propane are adsorbed only in the wide regions of the channels, while butane and *n*-pentane did not present any visible adsorption site and could move freely through the pores. The statistics of the molecule mass centre location for *n*-butane and *n*-pentane show that they occupy the centre of the pores and this would be an indicative that there is no adsorption site. The sorption capacity for *n*-pentane was about 15% higher than the experimental values of Newalkar et al. [5].

*Corresponding author. Email: lucena@ufc.br

ISSN 0892-7022 print/ISSN 1029-0435 online

DOI: 10.1080/08927020802301896
http://www.informaworld.com

Fox and Bates [12] studied the sorption of *n*-hexane and confirmed the molecule positioning suggested by Newalkar et al. [6]. However, the value for the simulated *n*-hexane concentration at saturation was almost 100% higher than the experimental values of Newalkar et al. [5] and Chiang et al. [7]. The concentration at saturation was calculated as 2 molecules/unit cell while the experimental data was about 1.1 and 1.18 [6,7] molecules/unit cell. There was no reference to adsorption sites.

Bhide and Yashonath [13] presented an interesting study of molecular dynamics of *n*-pentane in $AlPO_4$-5. According to the authors, when moving through the channel, the *n*-pentane molecule alternates its configuration from stretched to twisted (and *c*-axis orientation) as it passes through the narrow and wide pore regions, respectively. They also calculated the values for the adsorption heat at the wide and narrow channel regions. They showed that for the all-atom (AA) model used the heat of adsorption of *n*-pentane in the narrow region is about 2.5% higher than the heat of adsorption in the wide region.

In summary, some discrepancies emerged from the cited studies. While Newalkar et al. [5,6] consider that the *n*-pentane and *n*-hexane molecules are positioned parallel to the crystallographic *c*-axis, Bhide and Yashonath [13] evidenced that *n*-pentane molecules change from stretched to twisted configuration with different *c*-axis orientations when moving through the channel. Fox and Bates [12] calculated a saturation concentration for *n*-hexane as 2 molecules/unit cell, almost double the value observed experimentally. None of these studies established adsorption sites for the molecules.

In previous studies of xylenes isomers in aluminophosphate molecular sieves, we found that channel modulation, creating wide and narrow regions along the pores is a decisive factor for the adsorption properties of those molecules [14,15]. We have shown that for large cyclic molecules like xylenes, not only the wide pore region, but also the narrow region are adsorption sites. We also found that molecular positioning, adsorption sites and loading of cyclic hydrocarbons molecules vary remarkably depending on the force fields that are used [16].

Our objective in the present study is investigate the positioning, adsorption sites and loading of *n*-butane, *n*-pentane and *n*-hexane in $AlPO_4$-5 using the same approach of our pervious studies to gain insight into the adsorption behaviour of linear molecules in unidimentional pores and possibly contribute to clarify these discrepancies. With the choice of the sequence C4–C6, we can explore how the adsorption equilibrium changes with the growth of the molecular chain. The aluminophosphates one-dimensional channels offer a great perspective for this kind of structural analysis, because they represent the simplest topology of interconnected pores which are devoid of complications associated with higher dimensional channel systems.

Besides, we intend to study the questions related to the choice of force field, which can be a source of discrepancies in molecular simulations. We plan to evaluate a new AA force field developed in this study, united atom (UA) force fields used for linear alkanes [11,12] and the impact (on positioning and adsorption sites) of introducing dihedral angle rotation, a typical configurational biased move in UA models.

2. Simulation model

2.1 Structural details

The *n*-butane, *n*-pentane and *n*-hexane molecular structures were considered rigid in the AA models. Molecule flexibility is known to influence adsorption equilibrium. Smit and Siepmann [17], for example, have shown that for AA alkanes models from four to six carbons the intramolecular energy was about 10–15% of the intermolecular energy. In order to obtain a broad picture of this variable, we tested a rigid UA model to compare with the rigid AA model, and a flexible UA model to investigate the influence of flexibility in positioning and adsorption site. The flexible model can perform dihedral angle rotation as previously done by Bhide and Yashonath [13]. We also performed preliminary tests introducing dihedral angle rotation in AA model and only minimal molecular variation was evidenced.

$AlPO_4$-5 crystallises in the space group *P6/mcc* ($a = 13.8$ Å and $c = 8.45$ Å) with 72 atoms/unitary cell [18]. It forms one-dimensional pores with free diameter of 7.3 Å parallel to the crystallographic *c* direction (AFI structural network – hexagonal).

In aluminophosphates, the channels present distinct diameters. They exhibit diameter modulation along the *c*-axis, leading to alternate wide and narrow cross-sections. The narrow region is the ring oxygen windows and the wide region corresponds to the area of connections between two oxygen windows (see Figure 1).

$AlPO_4$-5 has narrow windows with 12 oxygen atoms with diameter of 9.96 Å and wide regions (connecting two consecutive windows) with diameter of 11.20 Å.

2.2 Interaction potentials

2.2.1 AA models

All interactions were modelled with a Lennard-Jones (LJ) potential given by:

$$U(r_{ij}) = 4\varepsilon_{ij}\left[\left(\frac{\sigma_{ij}}{r_{ij}}\right)^{12} - \left(\frac{\sigma_{ij}}{r_{ij}}\right)^{6}\right],$$

where ε_{ij} is the well depth, σ_{ij} is the diameter and r_{ij} is the distance between interacting atoms i and j.

As we do not have specific AA force fields for the system linear alkane/aluminophosphate, we had to set up a new group of parameters. For this, the LJ potentials between the hydrogen and oxygen atoms were taken from Bhide and Yashonath [19]. The C—C and H—H interaction parameters were taken from Jorgensen and Severance [20]. Finally, the

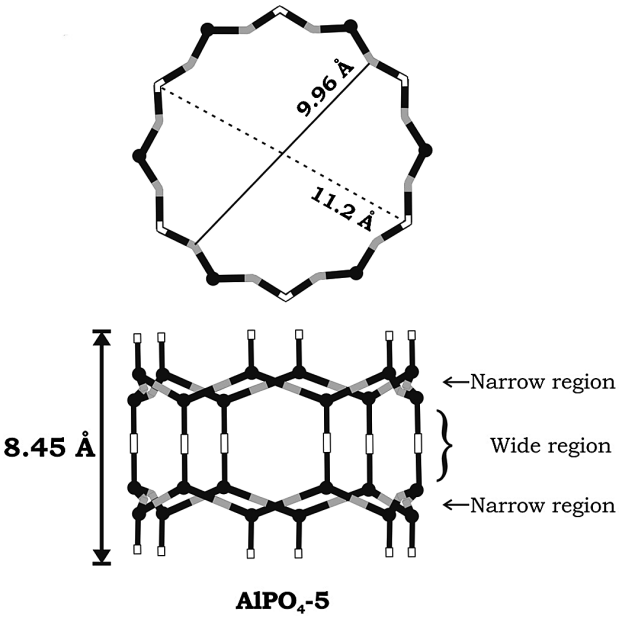

Figure 1. Cross-sectional and vertical view of the channels of $AlPO_4$-5. There are two diameters in the cross-sectional view, the narrow (9.96 Å) and the broad (11.20 Å). In the vertical view, we can see the different regions indicated along the channel. (Diameters are taken between oxygen atoms of the narrow and wide regions. Aluminum and phosphorus atoms, black balls; oxygen atoms in the windows, grey bars; oxygen atoms in the wide regions, white bars. Cross-sectional views represent one wide and one narrow plane.)

parameters ε_{ij} and σ_{ij} between carbon and oxygen atoms were adjusted so that the value of the *n*-butane-aluminophosphate interaction energy was close to the low loading adsorption heat value observed experimentally for *n*-butane in $AlPO_4$-5 [10]. The cross terms were obtained using arithmetic and geometric combination rules. The parameters are shown in Table 1. As usual, the interactions between Al and P atoms were ignored [21].

The validation of this force field was made through the calculation of the low loading heat of adsorption of linear and branched alkanes and subsequent comparison with the experimental values (Table 2). The heats of adsorption presented quite good agreement especially in the case of *n*-pentane and 2,3-dimethylbutane. Other important aspect is that the order of simulated values follows the same tendency revealed by the experimental data (2,3-dimethylbutane > *n*-hexane > 2-methylbutane > *n*-pentane).

Table 1. LJ potential parameters for AA models of linear alkanes.

	C[a]	H[a]	C—O[b]	H—O[c]
σ (Å)	3.55	2.42	3.00	2.71
ε (kcal mol^{-1})	0.07	0.03	0.223	0.068

[a] Jorgensen and Severance [17]. [b] This study. [c] Bhide and Yashonath [16].

Table 2. Experimental and simulated low loading adsorption for the AA force field.

	Experimental (kcal/mol)	Simulated (kcal/mol)
n-Hexane	13.5[a]; 14.3[b]	14.5
n-Pentane	12.4[c]	12.35
n-butane	10.5[b]	10.5
2-Methylbutane	13.0[c]	14.0
2,3- Dimethylbutane	15.8[a]	15.5

[a] Newalkar et al. [6]. [b] Eder and Lercher [18]. [c] Newalkar et al. [5].

2.2.2 *UA models*

All dispersion–repulsion forces were modelled using Lennard-Jones potentials.

In UA models a CH_3 or CH_2 group is represented by a single site located at the carbon atom position [17,22]. The advantage of UA force fields is that they are less time consuming for the calculations than the AA potential models.

The parameters for the UA models of *n*-butane and of *n*-pentane were obtained from Maris et al. [11]. In this study, the molecule–molecule parameters were obtained from the simulation of the liquid–vapour phase-equilibrium for *n*-heptane, 2-methylhexane and 3-ethylpentane [23]. The molecule-sieve parameters were optimised to reproduce Henry's constant and the heat of adsorption at low concentrations for several alkanes in silicalite. Despite being optimised for silicalite, the authors obtained good qualitative agreement using this force field in the simulations for $AlPO_4$-5.

The UA model of *n*-hexane was derived from the study by Fox and Bates [12]. The molecule–molecule parameters were obtained through the optimisation of the critical temperature and liquid-phase density of ramified alkanes from C4 to C8 [24]. The molecule-sieve parameters were the same parameters used by Maris et al. [11].

In the UA flexible model, dihedral angle rotation was included and occurs around C(2)—C(3); C(2)—C(3) and C(3)—C(4); C(2)—C(3), C(3)—C(4) and C(4)—C(5) bonds in *n*-butane, *n*-pentane and *n*-hexane molecules, respectively. The 'DRIEDING' potential [25] has been used:

$$E_{ijkl} = 1/2V_{jk}\left\{1 - \cos\left[n_{jk}\left(\varphi - \varphi^0_{jk}\right)\right]\right\},$$

where φ is the dihedral angle, n_{jk} is the periodicity, V_{jk} the barrier to rotation and φ^0_{jk} the equilibrium angle.

The parameters used in the UA models are presented in Table 3.

2.3 *Computational details*

The adsorption heats and isotherms calculations were performed in a simulation cell containing 27 unitary cells (3 × 3 × 3). The GCMC technique was used in the

Table 3. LJ and dihedral angle rotation parameters used in the UA models.

	n-Butane and *n*-pentane[a]		*n*-Hexane[b]	
Nonbounded	σ (Å)	ε (kcal mol^{-1})	σ (Å)	ε (kcal mol^{-1})
CH_3—CH_3	3.77	0.195	3.75	0.194
CH_2—CH_2	3.93	0.093	3.95	0.091
CH_3—O	3.6	0.159	3.6	0.159
CH_2—O	3.6	0.115	3.6	0.115
Torsion	n_{jk}	V_{jk} (kcal/mol)	φ^0_{jk} (rad.)	
CH_x—CH_2—CH_2—CH_x	2	45	1	

[a] Maris et al. [8]. [b] Fox and Bates [9].

adsorption isotherm simulations [26]. The algorithm allows displacements (translations and rotations), creations and destructions. These simulations consisted of evaluating the average number of adsorbate molecules for which the chemical potential equals that of the bulk phase at a given pressure and temperature.

In the low loading adsorption heat calculations we used a canonical ensemble Monte Carlo algorithm (fixed loading) with only four sorbate molecules in the simulation cell, with an initial choice of coordinates for the sorbate molecules, then allowing translations and rotations of the molecules until equilibrium is reached.

The UA simulations were done in a Dell p-390 workstation using the Sorption Module of Materials Studio® 4.1 [27]. The AA model simulations have been performed in a Silicon Graphics Inc. (SGI) Onyx2 station using Cerius[2] software suite [28]. Between 2 and 4 × 10^6 Monte Carlo steps were performed in order to calculate mean values. In order to check the convergence of our simulations, we have tested for some runs up to 9 × 10^6 Monte Carlo steps, without significant change in the results. The potentials cut off distance was 12 Å, which is in the same order of magnitude of previous studies in similar systems [29–31]. Each run lasted from 1 to 8 h of computing time depending on the simulated system. The UA models were up to four times quicker than the AA models.

3. Results and discussions

3.1 Adsorption isotherms

The adsorption isotherms of *n*-pentane and *n*-hexane in $AlPO_4$-5 were simulated at 30°C and compared with experimental data of Newalkar et al. (*n*-pentane and *n*-hexane) [5,6] and Chiang et al. (*n*-hexane) [7]. We did not find experimental adsorption isotherm for the *n*-butane in $AlPO_4$-5 in the open literature. In this case, we used the same temperature (30°C) used in the simulation of Maris et al. [11].

Figures 2 and 3 presents the simulated and the experimental isotherms for *n*-hexane and *n*-pentane. As previously observed for cyclic molecules, the experimental adsorbed phase concentration for linear alkanes reaches about 80–90% of the total sorption capacity still at very low pressures ($P/P_0 \sim 0.01$) [3].

In Figure 2, we can observe that the results for the *n*-hexane AA model showed fine agreement with the experimental values [7]. However, the UA rigid model presented values 18% smaller than the experimental ones

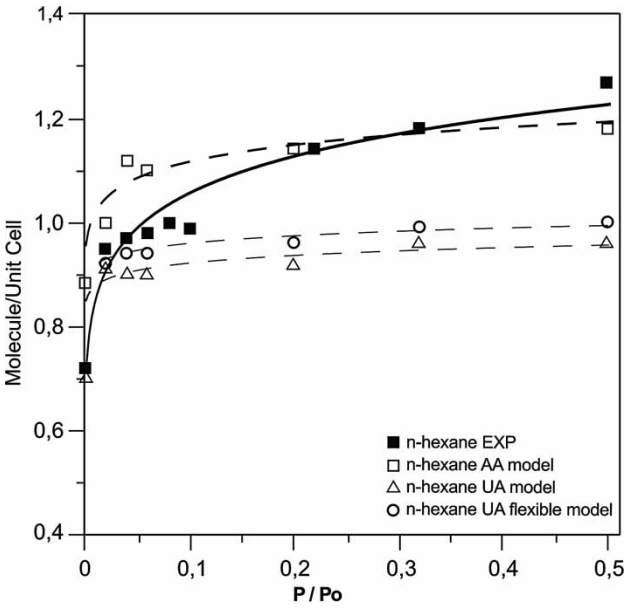

Figure 2. Adsorption isotherms of *n*-hexane in $AlPO_4$-5 at 30°C ($P_0 = 24$ kPa). Our simulation (dashed lines and open symbols) and experimental data [25] (solid lines and symbols).

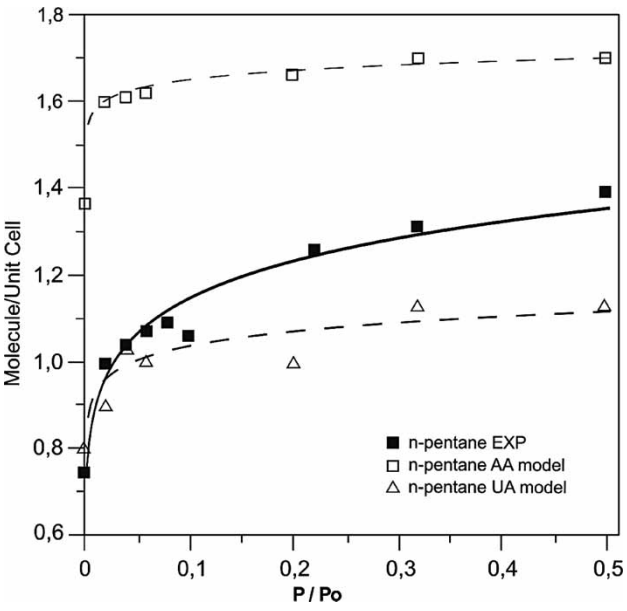

Figure 3. Adsorption isotherms of *n*-pentane in $AlPO_4$-5 at 30°C ($P_0 = 81$ kPa). Our simulation (dashed lines and open symbols) and experimental data [24] (solid lines and symbols).

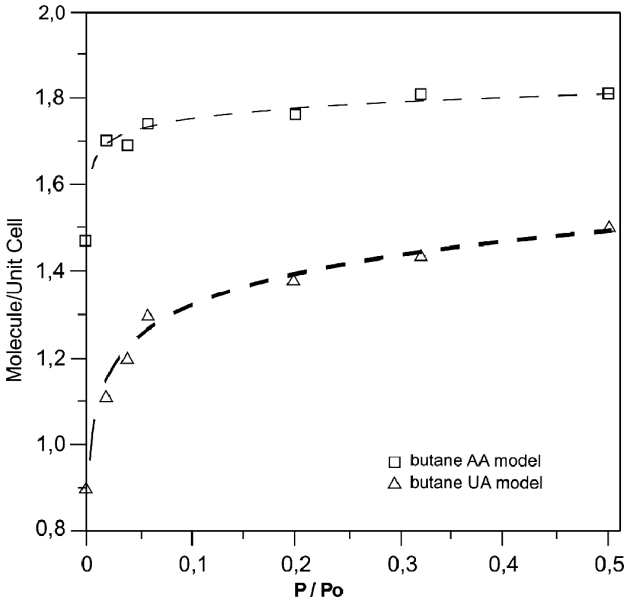

Figure 4. Simulated adsorption isotherms for *n*-butane in $AlPO_4$-5 at 30°C ($P_0 = 282$ kPa).

for $P/P_0 = 0.5$ (0.96 molecules/unit cell). Also in Figure 2 the results for the UA flexible model isotherm are shown for comparison.

In spite of using the same nonbonded parameters, the loading values found for the UA model in our simulation are completely different from the ones calculated by Fox and Bates [12]. This difference cannot be attributed to the use of a biased algorithm scheme. In the next subsection (structural analysis), we will proceed with this discussion.

For *n*-pentane adsorption in $AlPO_4$-5, we observe more disperse results (Figure 3). While the AA values exceeds in 20% the experimental value at $P/P_0 = 0.5$ [3], the value for the UA rigid model is approximately 20% lower than the experimental value for the same pressure ratio.

In Figure 4, the simulated isotherms of the models for *n*-butane are shown. These values can be used only in comparison with simulated *n*-pentane and *n*-hexane isotherms, since we do not have *n*-butane experimental data. Again the AA model presents higher adsorbed phase concentrations than the UA rigid model. The loading values of the AA rigid model are very close to the UA flexible model of Maris et al. [11].

The UA rigid force field yielded values for the heat of adsorption in low concentrations of 7.6, 8.8 and 10.3 kcal/mol for *n*-butane, *n*-pentane and *n*-hexane, respectively. For the same molecules, the UA flexible model presented low loading heats of adsorption of 7.8, 8.9 and 10.7 kcal/mol, respectively.

3.2 Structural analysis: molecular positioning and adsorption sites

The structural analysis methodology for the linear molecules was similar to what was applied in a previous study [16]. The molecular positioning was monitored by the angle formed between the end-to-end distance (measured between the terminal groups of the molecules) and the crystallographic *c*-axis. The adsorption sites were determined based in the statistics of mass centres of the molecules during the sampling of the configurations in the grand canonical ensemble.

3.2.1 n-*Hexane*

Figure 5 presents the distribution of probability of the angles for *n*-hexane in the AA and UA models. We observe a coincidence of positioning for the two models. The molecules are approximately parallel to the channels of the aluminophosphate (angles from 30° to 40°). This positioning coincides partially with what was proposed

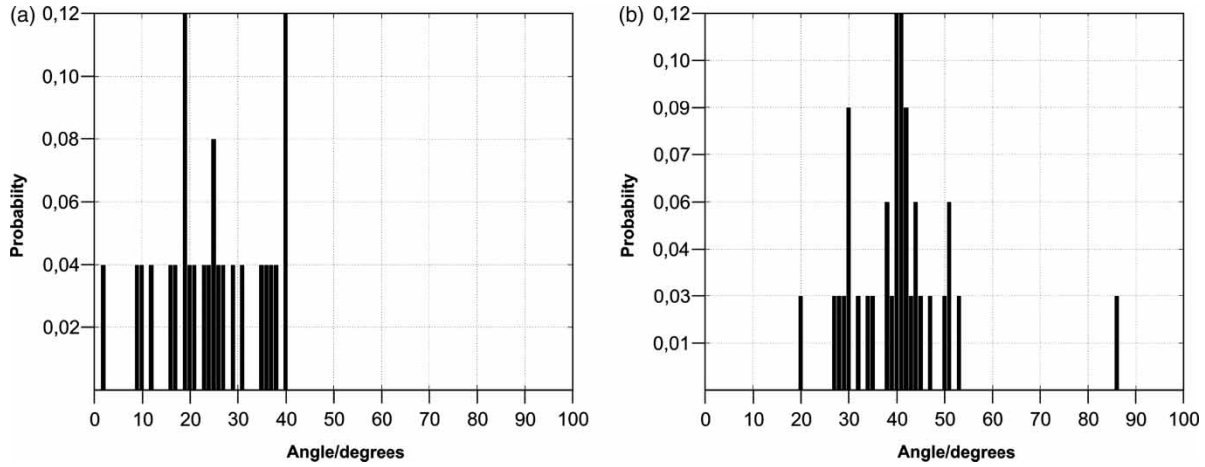

Figure 5. Probabilities for the angle between the molecule end-to-end vector and the crystallographic *c*-axis at high loadings for *n*-hexane (a) AA model and (b) UA model. The angle values are mainly in the low range (vertical positioning).

by Newalkar et al. [6]. In spite of the molecules being found mostly in the position parallel to the *c*-axis, it is clear that they did not need to assume a twisted position to achieve the value of the experimental loading. As the wide region diameter is on average 1.0 Å larger than the narrow region diameter, the molecule with its mass centre located in the narrow region has more room to tilt obtaining a loading of 1.18 molecules/unit cell without necessarily assuming a twisted position.

The introduction of dihedral angle rotation in the molecule did not alter significantly the end-to-end distance nor the positioning. The end-to-end equilibrium distance that was 6.4 Å in the optimised rigid molecule changes to a minimum value of 5.8 Å. The average value was 6.2 Å.

Figure 6 shows the distribution of the mass centres indicating the pore narrow regions as adsorption sites in both force fields. We can also observe that the narrow regions are visited with more frequency in the UA model than in the AA model. This indicates a smaller activation energy in the UA model so the molecules can move more freely. As mentioned, the introduction of dihedral angle rotation in the molecule did not alter the adsorption sites as seen in Figure 7.

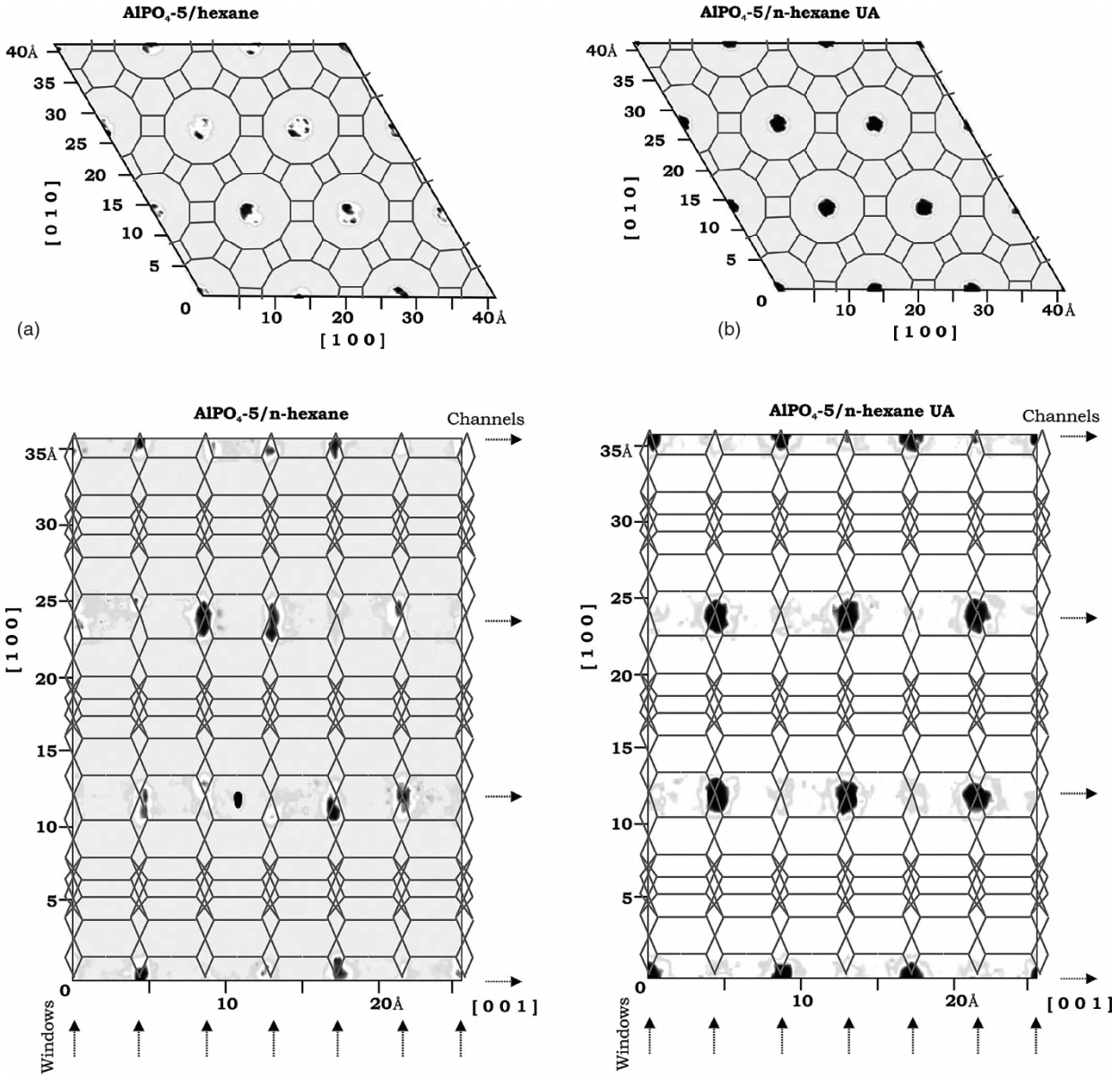

Figure 6. View of the 3 × 3 × 3 simulation cell of $AlPO_4$-5 and *n*-hexane with respective statistics of mass centres location of the success moves during simulation for (a) AA model and (b) UA model. Superior view is projected down plane (0 0 1) and side view is projected down plane (0 1 0). Dark areas are of high mass centres occurrence. We can observe the positioning of *n*-hexane in the narrow region (windows) for both models.

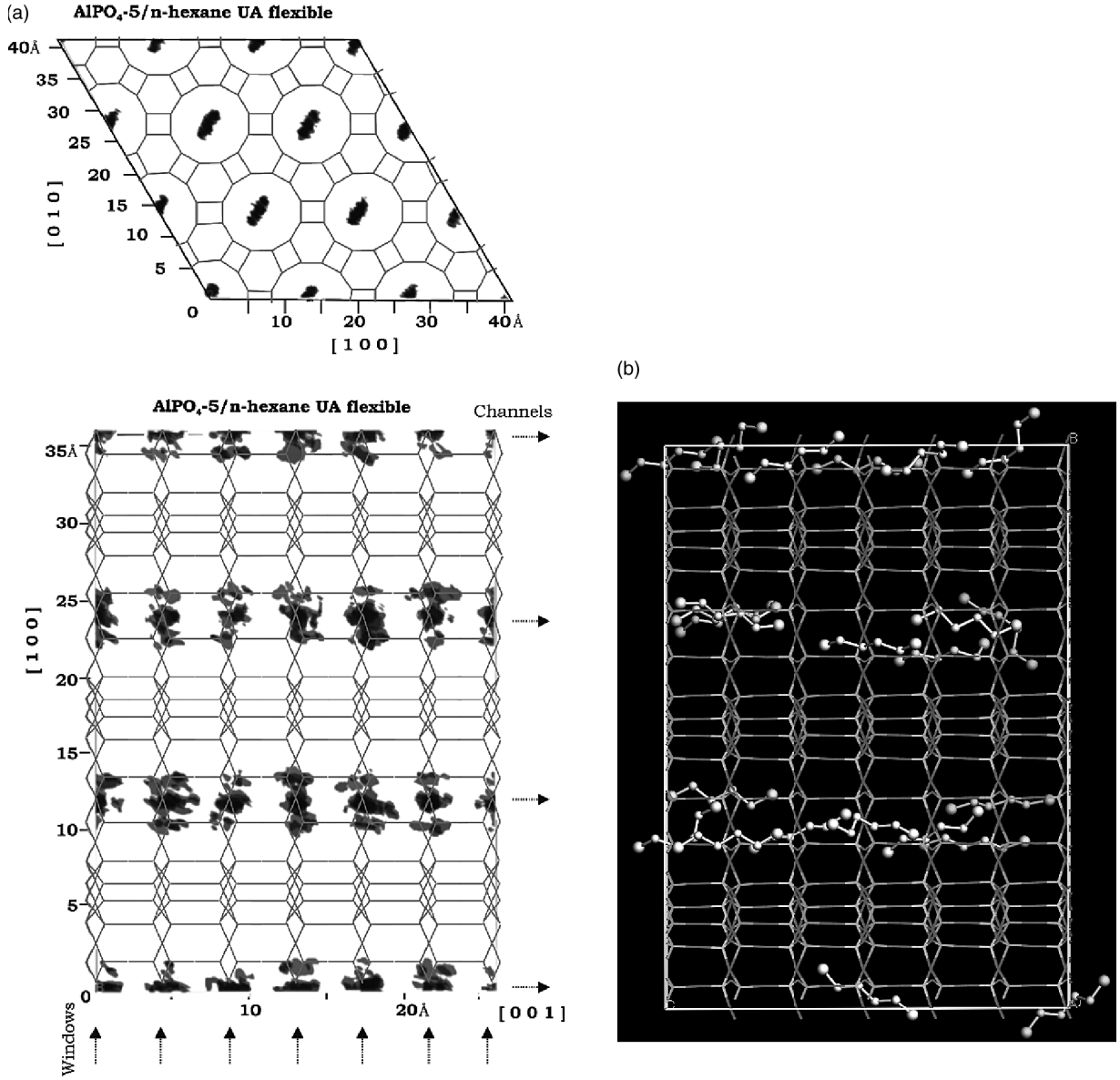

Figure 7. (a) View of the 3 × 3 × 3 simulation cell of $AlPO_4$-5 and *n*-hexane with respective statistics of mass centres location of the success moves during simulation for UA flexible model and (b) lateral view of the simulation cell with UA flexible model, showing *n*-hexane molecules centred in narrow regions (windows).

In the structural analyses, for *n*-hexane and the other linear alkanes, we noticed a strong interaction between the terminal methyl radicals and the oxygen atoms of the wide region. This kind of strong interaction was also identified in our previous study for xylenes methyl groups [12].

Bhide and Yashonath [13], in their study of molecular dynamics with *n*-pentane, evaluated the average potential energy for the interacting groups —CH_2 and —CH_3. They found that while each —CH_3 group contributed with 5.5 kcal/mol each —CH_2 group contributed approximately with only 2.8 kcal/mol. This strong terminal group interaction is what determines the angle of inclination of the *n*-hexane molecules. So, once positioned in the narrow region, the molecule assumes a sloping position to optimise the —CH_3/O interaction. This interaction results in an average methyl–oxygen equilibrium distance of 3.8 Å for *n*-hexane (see Figure 8).

Now, in the light of structural analysis, we can make some additional observations about the discrepancy between the simulated data from Fox and Bates [9] and the results we obtained in this study. Each unit cell of $AlPO_4$-5 has only one pore with diameter 7.3 Å and length 8.45 Å. The dimensions of the *n*-hexane molecule, in the minimum energy state (linear), are 10.3 Å length and 4.53 Å diameter [32].

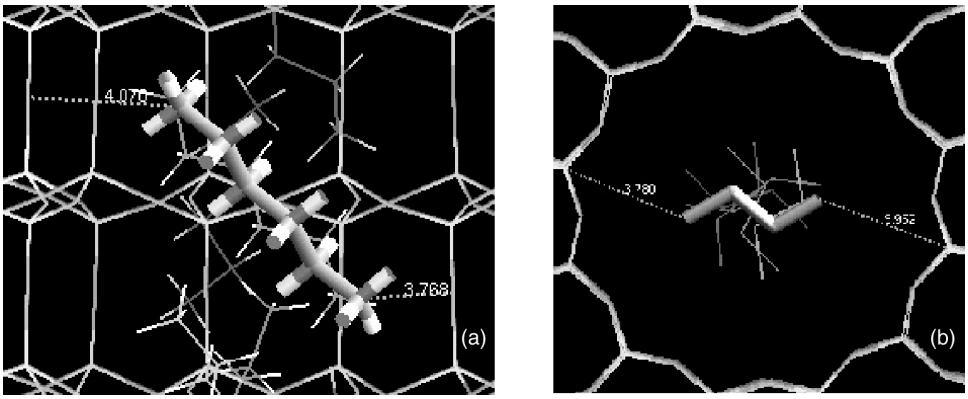

Figure 8. (a) Lateral view of the pore with *n*-hexane molecules adsorbed in $AlPO_4$-5, showing the suggested vertical dominant pattern centred in narrow regions (windows). The molecule presents a tilted configuration in function of the $-CH_3/O$ strong interaction. (b) Superior view of the pore with *n*-butane molecules showing the suggested horizontal dominant positioning centred in wide regions. These positionings are the same for rigid and flexible models. Typical methyl–oxygen equilibrium distances are shown (dashed lines).

When the molecule tilts to maximise the interaction methyl–oxygen it improves its packing occupying approximately 7.7 Å of the linear length of the pore (supposing a tilting medium angle of 40° in the AA model – see Figure 5). This allows concentrations slightly above 1 molecule/unit cell. The length of the molecule decreases only to 9.4 Å with the introduction of dihedral angle rotation. This happens because, as described above, the methyl terminals are strongly attracted by the oxygen of the wide region not favouring the most twisted configurations. If we suppose that the molecule can assume more twisted configurations, a larger degree of torsion would increase the diameter of the molecule causing a decrease in the tilting angle and consequently in the packing. The only physically possible way for the unit cell pore to accommodate two molecules would be if they could be placed side by side. This is not possible since the pore diameter is only 7.3 Å.

3.2.2 n-*Butane*

Figure 9 shows the distribution of probability of the angles for *n*-butane in the AA and UA models. The distribution is more uniform for the AA model and presents a larger dispersion for the UA rigid model. In both models the horizontal position for the molecules (approximately perpendicular to the *c*-axis) prevails. The analysis of the statistics of mass centres (Figure 10) shows for both models the wide regions as adsorption sites. The introduction of dihedral angle rotation in the UA model did not alter the adsorption sites nor the positioning. Again, in all models the positioning is influenced by the strong interactions between the terminal methyl groups and the oxygen atoms of the wide region. This interaction results in an average equilibrium methyl–oxygen distance of 3.5 Å (Figure 8(b)). The smallest dispersion of the horizontal positions in the AA model can explain the larger

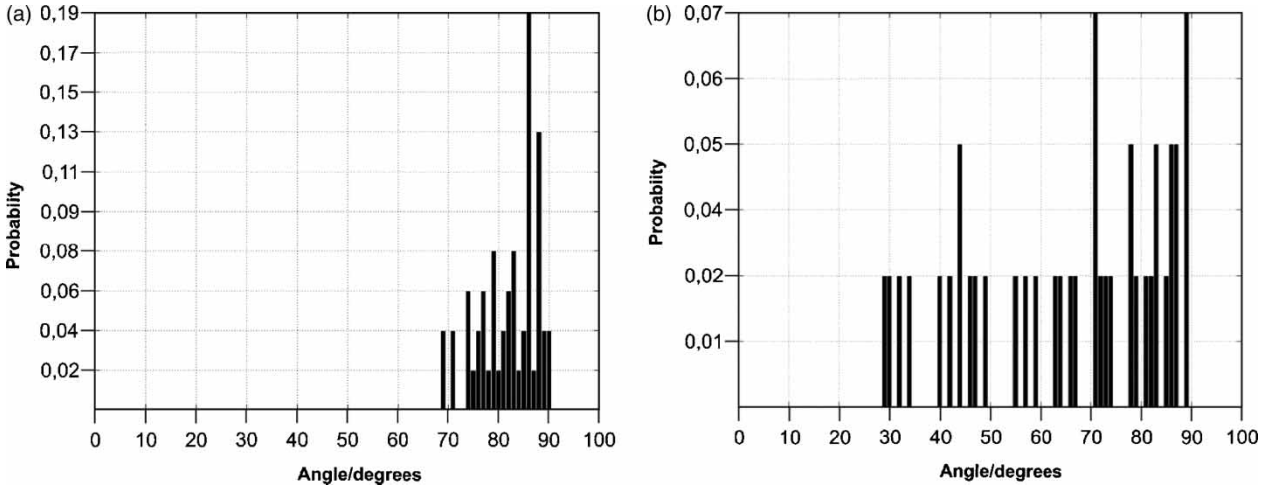

Figure 9. Probabilities for the angle between the molecule end-to-end vector and the crystallographic *c*-axis at high loadings for *n*-butane (a) AA model and (b) UA model. The angle values are mainly in the high range (horizontal positioning).

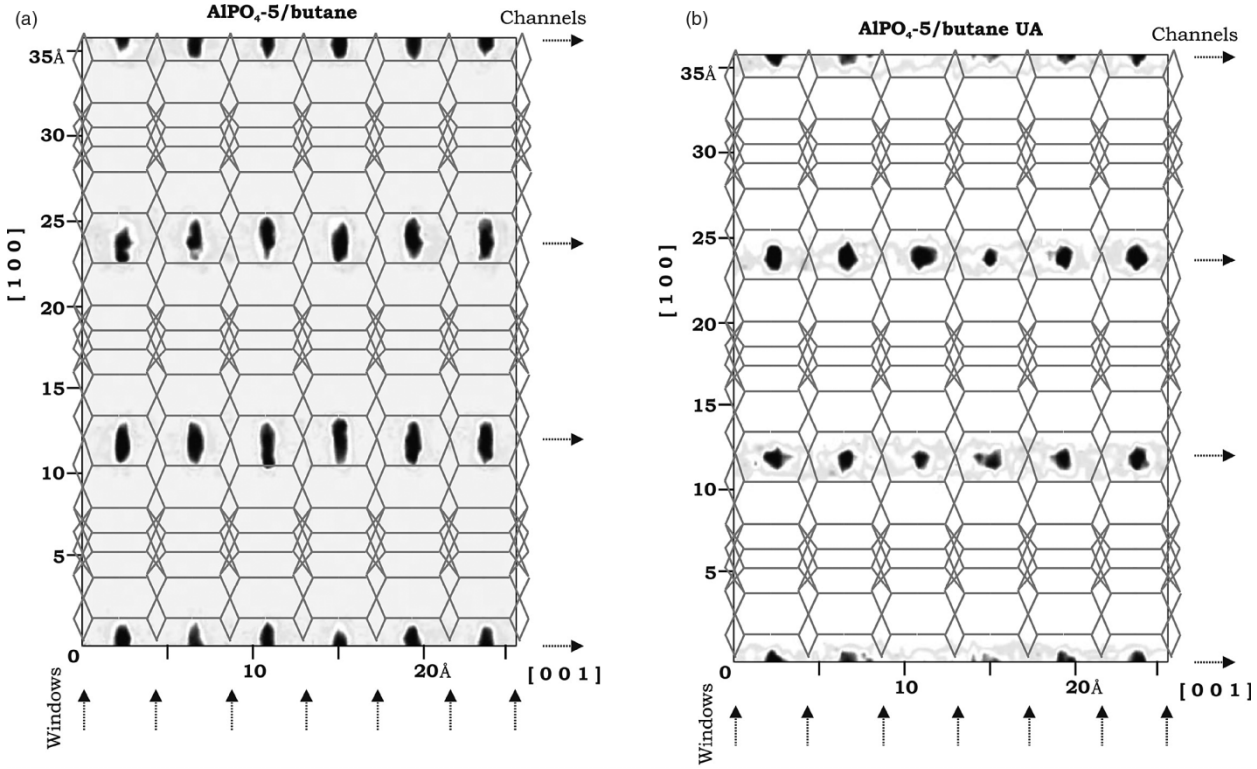

Figure 10. Side view of the 3 × 3 × 3 simulation cell of $AlPO_4$-5 and *n*-butane with respective statistics of mass centres location of the success moves during simulation for (a) AA model and (b) UA model. Simulation cells are projected down plane (0 1 0). Dark areas are of high mass centres occurrence. We can observe the positioning of *n*-butane in the wide region for both models.

values of concentration observed in the simulated adsorption isotherm.

3.2.3 n-*Pentane*

The *n*-pentane molecules present a complex behaviour. While in the AA model the distribution of probability of angles shows that the molecules are positioned almost perpendicular to the axis *c* (horizontal positioning), for the UA model they are in the vertical position (Figure 11). The analysis of the statistics of mass centres also presents divergent results between the two force fields (Figure 12). While in the AA model the wide regions are clearly defined as adsorption sites, for the model UA it is not

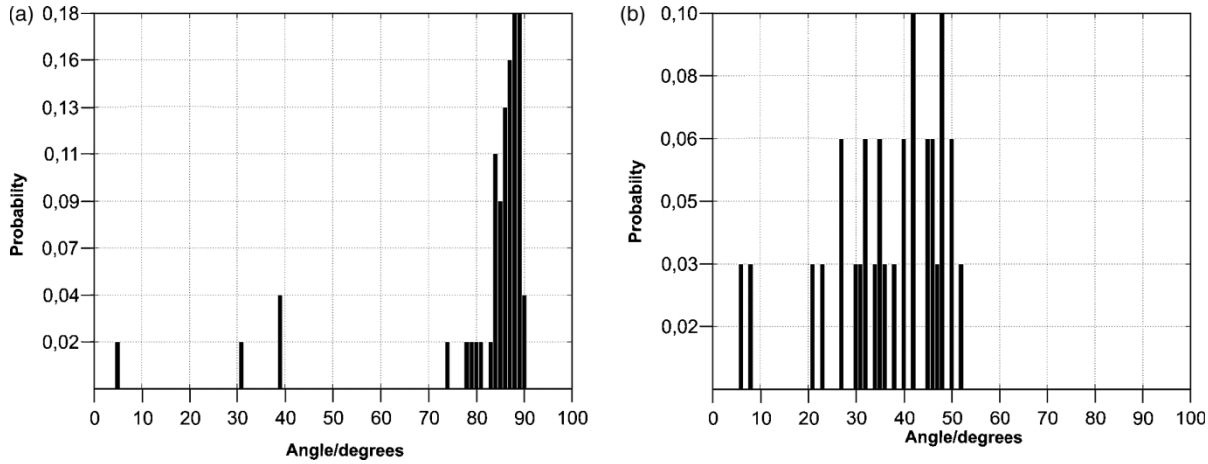

Figure 11. Probabilities for the angle between the molecule end-to-end vector and the crystallographic *c*-axis at high loadings for *n*-pentane (a) AA model and (b) UA model. In the AA model, the angle values are mainly in the high range (horizontal positioning) while in UA model low angles are dominant (vertical positioning; I).

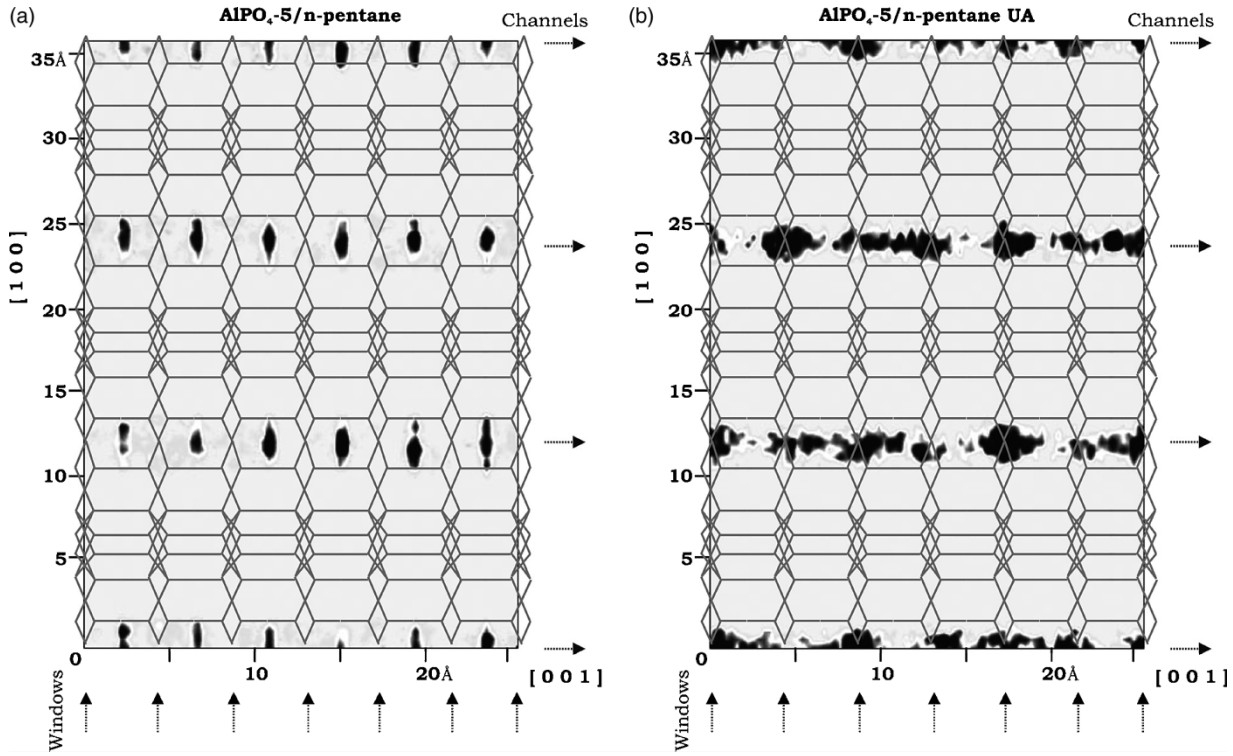

Figure 12. Side view of the 3 × 3 × 3 simulation cell of $AlPO_4$-5 and *n*-pentane with respective statistics of mass centres location of the success moves during simulation for (a) AA model and (b) UA model. Simulation cells are projected down plane (0 1 0). Dark areas are of high mass centres occurrence. While in the AA model the wide regions are clearly defined as adsorption sites, in the UA model we can not clearly identify adsorption sites.

possible to define the adsorption sites, in agreement with previous results reported by Maris et al. [11]. The torsion moves introduced in the flexible UA model did not alter position and adsorption sites.

The horizontal packing of the AA model is responsible for the higher adsorbed phase concentration values that was observed in the adsorption isotherm (Figure 3). On the contrary, the vertical positioning of the UA model induces a smaller amount of adsorbed molecules. In the case of the UA flexible model used by Maris et al. [11] the possibility of the molecule inhabiting any area of the pore associated the torsion and bend freedom, adjusting angles and lateral growth, and should have resulted in the adsorption simulated values of 15% more than the experimental value of Newalkar et al. [5].

We also performed low concentration simulations of the AA model (up to 10 molecules/unit cell) that resulted in preference for the vertical positioning (65% of the molecules) similar what was suggested by the UA model. With a small increase of the concentration, the high angle horizontal positioning is favoured and prevails within the crystal. This type of orientation change did not happen for *n*-hexane or *n*-butane molecules. A typical image of the *n*-pentane two dominant positions in AA and UA models is shown in Figure 13.

3.2.4 Levitation effect

For *n*-pentane, we found the largest divergence between the two models of force fields. It diverges in the adsorbed phase concentrations in the isotherms, in the positioning of the molecules and in the location of the sites of adsorption.

These large differences in the properties of *n*-pentane using different force fields led us to search, in the series of alkane molecules studied, for evidence of the levitation effect as previously found for cyclic molecules [16].

Levitation effect is a critical geometric condition identified by Yashonath and co-workers [19,33–35] in molecular dynamics studies for diffusion anomalies in molecular sieves. In this condition, the net forces on the guest due to the host is at a minimum, the levitation ratio (γ) is close to unity and there is a weakly bound guest that can be easily moved from its equilibrium position. This effect, identified first in spherical monoatomic guest species [33,35] was extended to linear molecules by Ghorai et al. [34].

n-Pentane that showed results that were more affected by the choice of force field would probably have dimensions that would result in levitation ratios (γ) close to unity. On the other hand, *n*-hexane and *n*-butane, which is only slightly affected by the choice of force field, should have levitation ratio different from unity.

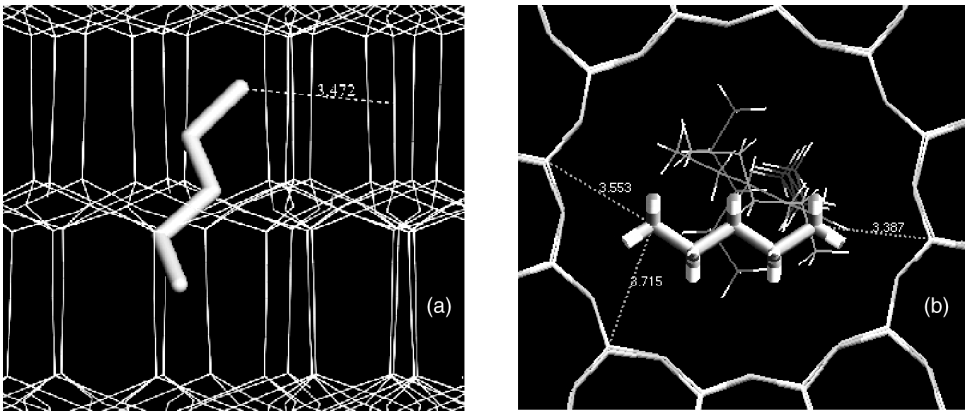

Figure 13. (a) Lateral view of the pore with molecules of *n*-pentane (UA model) adsorbed in $AlPO_4$-5, showing the suggested vertical dominant pattern centred in the narrow regions (windows). (b) Superior view of the pore with molecules of *n*-pentane (AA model) showing the suggested horizontal dominant positioning centred in wide regions. All these positionings are the same for the rigid and the flexible models. Typical methyl–oxygen equilibrium distances are shown (dashed lines).

To test this possibility, we used the equation proposed by Ghorai et al. [34] for the levitation ratio:

$$\gamma = \frac{2^{7/6}\sigma_{gh} + l}{\sigma_w},$$

where σ_{gh} is the hydrogen–oxygen (guest–host) interaction parameter, σ_w is the window diameter defined as the centre-to-centre distance between diagonal oxygen atoms of the channel and l is the end-to-end distance between the atomic centres of the linear guest.

In Table 4, we show the values of the calculated parameters for $AlPO_4$-5 and the respective adsorbate molecules from our AA model data. We observe that *n*-pentane presents levitation ratio value of 0.99 while *n*-butane and *n*-hexane show levitation ratios different from unity (0.88 and 1.12, respectively).

Similar to the study for the cyclic molecules, this can be the cause of the discrepancy found in the adsorption isotherm, positioning and adsorption sites between the different force fields that were used to simulate the adsorption equilibrium of *n*-pentane molecules.

4. Conclusions

n-Hexane molecules locate parallel to the crystallographic *c*-axis as suggested by the experimental data of Newalkar et al. [6] and the simulations of Fox and Bates [12]. We demonstrated that the angle of inclination of the molecules is determined by the optimised distance —CH_3/O and that the preferential adsorption site locates in the narrow region. Contrary to previous suppositions of Newalkar et al. [6] and Chiang et al. [7], the *n*-hexane molecule did not need to assume a twisted position to achieve the experimental loading as demonstrated by the good agreement between the simulated isotherm using the AA model and the experimental data [7]. We applied the same group of parameters used by Fox and Bates [12] in the simulation using the UA model obtaining a maximum adsorbed phase concentration of only 0.96 molecules/unit cell versus 2.0 in the simulation performed by those authors. The reasons for this discrepancy is not clear. Based in the structural analysis we conclude that 2 molecules/unit cell seems difficult to achieve in the $AlPO_4$-5 pores.

Table 4. Dimensions and levitation ratios for *n*-hexane, *n*-pentane and *n*-butane (from the AA model data).

	σ_w (Å)	σ_{gh} (Å)	l (Å)	γ
n-Butane	11.2	2.71	3.8	0.88
n-Pentane	11.2	2.71	5.1	0.99
n- Hexane	11.2	2.71	6.5	1.12

For *n*-butane, the positioning was predominantly horizontal in both AA and UA model. The narrow region was clearly defined as adsorption site in all models.

Larger discrepancies between the force fields were found during the evaluation of the equilibrium data of *n*-pentane. Our simulations with the AA model evidenced a new pattern of horizontal positioning that prevails at high loading. The AA model also presented the vertical pattern suggested by Newalkar et al. [6] and Fox and Bates [12] but it just occurs in the low loading range. We observed that for the UA model there is only the vertical pattern. While in the AA model the wide regions are clearly defined as adsorption sites, for the UA model it was not possible to define the adsorption sites. Both AA and UA force fields were incapable to reproduce the experimental adsorption isotherm.

The critical geometric condition denominated levitation effect can explain the great sensibility of *n*-pentane for the different force fields. The estimated levitation ratios of *n*-butane, *n*-pentane and *n*-hexane molecules show that

n-pentane had levitation ratio close to unity, while the other two molecules presented values different from unity. This is, to our knowledge, the first time that a Monte Carlo molecular simulation study shows an evidence of the levitation effect in linear molecules.

It should also be noted that for both tested models (AA and UA) a strong interaction between the terminal methyl groups and the oxygen atoms of the wide regions was observed. This interaction influenced positioning and adsorption sites for all linear molecules studied.

Finally, in spite of the fact that AA models are considered more precise than UA models, for molecules with the range of sizes studied in this paper (*n*-butane to *n*-hexane) being adsorbed in one-dimensional pores, we observed that the full AA models presented identical values of adsorption sites and similar positioning as the UA models. Therefore, the use of UA models would be more interesting because of the lower computational effort. It would be also worth noting that for larger molecules the use of rigid models could be unfeasible, particularly in sieves with three-dimensional pores. This would happen for two reasons. Firstly the increase in chain length of the molecules can bring difficulties to the insertion/deletion moves in the GCMC scheme. Secondly, if the molecules had lengths larger than the distance between intersections, they would bend from one channel type to another.

Acknowledgements

The authors wish to acknowledge financial support for this study from CAPES, CNPq and FINEP/CTPETRO. We are also grateful to Professor Randy Snurr (Northwestern University, USA) for rich discussions on molecular simulations shared during S.M. Lucena's short sabbatical stay with his group.

Note

1. Email: celio@gpsa.ufc.br

References

[1] I.E. Maxwell and W.H.J. Stork, *Hydrocarbon processing with zeolites*, in *Introduction to Zeolite Science and Practice*, H. Van Bekkum, ed., Elsevier, Amsterdam, 1991, pp. 571–628.

[2] D.M. Ruthven, *Principles of Adsorption and Adsorption Processes*, John Wiley & Sons, New York, 1984.

[3] S. Raghuram and S.A. Wilcher, *The separation of* n-*paraffins from paraffin mixtures*, Sep. Sci. Technol. 27 (1992), pp. 1917–1954.

[4] M. Mazzotti, R. Baciocchi, S. Giuseppe, and M. Morbidelli, *Vapor-phase SMB adsorptive separation of linear/nonlinear paraffins*, Ind. Eng. Chem. Res. 35 (1996), pp. 2313–2321.

[5] B.L. Newalkar, R.V. Jasra, V. Kamath, and S.G.T. Bhat, *Sorption of* n-*pentane, 2-methylbutane and cyclopentane in microporous $AlPO_4$-5*, Microporous Mater. 11 (1997), pp. 195–205.

[6] B.L. Newalkar, R.V. Jasra, V. Kamath, and S.G.T. Bhat, *Sorption of C6 alkanes in aluminophosphate molecular sieve, $AlPO_4$-5*, Adsorption 5 (1999), pp. 345–357.

[7] A.S.T. Chiang, C.K. Lee, and Z.H. Chang, *Adsorption and diffusion of aromatics in $AlPO_4$-5*, Zeolites 11 (1991), pp. 380–386.

[8] C.L. Cavalcante, Jr, D.C.S. Azevedo, I.G. Souza, A.C.M. Silva, O.L.S. Alsina, V.E. Lima, and A.S. Araujo, *Sorption and diffusion of p-xylene and o-xylene in aluminophosphate molecular sieve $AlPO_4$-11*, Adsorption 6 (2000), pp. 53–59.

[9] J. Jänchen, H. Stach, L. Uytterhoeven, and W.J. Mortier, *Influence of the framework density and effective electronegativity of silica and aluminophosphate molecular sieves on the heat of adsorption of nonpolar molecules*, J. Phys. Chem. 100 (1996), pp. 12489–12493.

[10] F. Eder and J.A. Lercher, *Alkane sorption on siliceous and aluminophosphate molecular sieves. A comparative study*, J. Phys. Chem. 100 (1996), pp. 16460–16462.

[11] T. Maris, T.J.H. Vlugt, and B. Smit, *Simulation of alkane adsorption in the aluminophosphate molecular sieve $AlPO_4$-5*, J. Phys. Chem. B 102 (1998), pp. 7183–7189.

[12] J.P. Fox and S.P. Bates, *Simulating the adsorption of linear, branched and cyclic alkanes in silicalite-1 and $AlPO_4$-5*, Micro Meso. Mater. 69 (2004), pp. 9–18.

[13] S.Y. Bhide and S. Yashonath, n-*Pentane and isopentane in one-dimensional channels*, J. Am. Chem. Soc. 125 (2003), pp. 7425–7434.

[14] S.M.P. Lucena, J.A.F.R. Pereira, and C.L. Cavalcante, Jr, *Structural analysis and adsorption sites of xylenes in $AlPO_4$-5 and $AlPO_4$-11 using molecular simulation*, Micro Meso. Mater. 88 (2006), pp. 135–144.

[15] S.M.P. Lucena, J.A.F.R. Pereira, and C.L. Cavalcante, Jr, *Ortho-selectivity in aluminophosphate molecular sieves: A molecular simulation study*, Adsorption 12 (2006), pp. 423–434.

[16] S.M.P. Lucena, J.A.F.R. Pereira, and C.L. Cavalcante, Jr, *Sensitivity to guest–host force fields in adsorption equilibrium of cyclic hydrocarbons in one-dimensional molecular sieve*, Mol. Simul. 33 (2007), pp. 437–448.

[17] B. Smit and J.I. Siepmann, *Computer simulations of the energetics and siting of* n-*alkanes in zeolites*, J. Phys. Chem. 98 (1994), pp. 8442–8452.

[18] J.M. Bennet, J.P. Cohen, E.M. Flanigen, J.J. Pluth, and J.V. Smith, *Crystal structure of tetrapropylammonium hydroxide–aluminum phosphate*, Number 5, ACS Symp. Ser. 218 (1983), pp. 109–118.

[19] S.Y. Bhide and S. Yashonath, *Structure and dynamics of benzene in one-dimensional channels*, J. Phys. Chem. B 104 (2000), pp. 11977–11986.

[20] W.L. Jorgensen and D.L. Severance, *Aromatic–aromatic interactions: Free energy profiles for the benzene dimer in water, chloroform, and liquid benzene*, J. Am. Chem. Soc. 112 (1990), pp. 4768–4774.

[21] A.V. Kiselev, A.A. Lopatkin, and A.A. Shulga, *Molecular statistical calculation of gas adsorption by silicalite*, Zeolites 5 (1985), pp. 261–267.

[22] J.I. Siepmann, S. Karaborni, and B. Smit, *Simulating the critical behaviour of complex fluids*, Nature 365 (1993), pp. 330–332.

[23] J.I. Siepmann and M.G. Martin, *Intermolecular potentials for branched alkanes and the vapour–liquid phase equilibria of* n-*heptane, 2-methylhexane, and 3-ethylpentane*, Mol. Phys. 90 (1997), pp. 687–694.

[24] M.G. Martin and J.I. Siepmann, *Novel configurational-bias Monte Carlo method for branched molecules. Transferable potentials for phase equilibria. 2. United-atom description of branched alkanes*, J. Phys. Chem. B 103 (1999), pp. 4508–4517.

[25] S.L. Mayo, B.D. Olafson, and W.A. Goddard, *DREIDING: A generic force field for molecular simulations*, J. Phys. Chem. 94 (1990), pp. 8897–8909.

[26] D. Frenkel and B. Smit, *Understanding Molecular Simulation*, Academic Press, New York, 2002.

[27] Sorption, invoked from *Materials Studio v. 4.1*, Accelrys Inc., San Diego, (2007).

[28] Sorption, invoked from *Cerius^2 v. 4.6*, Accelrys Inc., San Diego, (2001).

[29] R.Q. Snurr, A.T. Bell, and D.N. Theodorou, *Prediction of adsorption of aromatic hydrocarbons from grand canonical Monte Carlo simulations with biased insertions*, J. Phys. Chem. 97 (1993), pp. 13742–13752.

[30] R.Q. Snurr, A.T. Bell, and D.N. Theodorou, *Molecular simulations of low occupancy adsorption of aromatics in silicalite*, Proc. Ninth Int. Zeolite Conf. II (1993), pp. 71–78.
[31] S.B. McCullen, P.T. Reischman, and D.H. Olson, *Hexane and benzene adsorption by aluminophosphates and SSZ-24: The effect of pore size and molecular sieve composition*, Zeolites 13 (1993), pp. 641–644.
[32] C.E. Webster, R.S. Drago, and M.C. Zerner, *A method for characterizing effective pore sizes of catalysts*, J. Phys. Chem. B 103 (1999), pp. 1242–1249.
[33] S. Yashonath and P. Santikaryt, *Diffusion of sorbates in zeolites Y and A: Novel dependence on sorbate size and strength of sorbate–zeolite interaction*, J. Phys. Chem. 98 (1994), pp. 6368–6376.
[34] P.Kr. Ghorai, S. Yashonath, P. Demontis, and G.B. Suffritti, *Diffusion anomaly as a function of molecular length of linear molecules: Levitation effect*, J. Am. Chem. Soc. 125 (2003), pp. 7116–7123.
[35] S. Bandyopadhyay and S. Yashonath, *Diffusion anomaly in silicalite and VPI-5 from molecular dynamics simulations*, J. Phys. Chem. 99 (1995), pp. 4286–4292.